

Figure S1

Figure S1. A β RA-LTMRs innervating the hair follicle, Meissner corpuscle, and Pacinian corpuscle all encode dynamic stimuli and express Piezo2, related to Figure 1.

(A) In vivo recording of an A β RA-LTMR forming lanceolate endings from an *NPY2R-GFP* mouse in response to step indentations and 100 Hz vibration delivered to the center of the receptive field of hairy thigh skin. Similar responses were observed in five GFP⁺ cells of four *NPY2R-GFP* mice.

(B) In vivo recording of a representative A β RA-LTMR unit innervating a Meissner corpuscle in response to step indentation and 100 Hz vibration delivered to the center of the receptive field on glabrous hindpaw.

(C) In vivo recording of a representative A β RA-LTMR unit innervating a Pacinian corpuscle in response to step indentation and 100 Hz vibration delivered to the ankle.

(D) Distance traveled in open field test for *Piezo2^{smFP-FLAG}/*Piezo2^{smFP-FLAG}** animals (n = 4), *Piezo2^{smFP-FLAG}/+* animals (n = 7), and wild-type littermates (n = 5). There were no statistically significant differences between group means as determined by one-way ANOVA (F (2, 13) = 2.538, p = 0.1174).

(E) Total time it took for *Piezo2^{smFP-FLAG}/*Piezo2^{smFP-FLAG}** animals (n = 4), *Piezo2^{smFP-FLAG}/+* animals (n = 7), and wild-type littermates (n = 5) to cross the balance beam. There were no statistically significant differences between group means as determined by one-way ANOVA (F (2, 13) = 0.07733, p = 0.9260). Mean \pm SEM. Each dot represents an animal.

(F) Piezo2-FLAG protein localizes to the NFH⁺ A β RA-LTMRs forming lanceolate endings in hairy skin, Meissner corpuscles in glabrous skin, and the Pacinian corpuscle and co-localizes with protrusion-like processes along the A β RA-LTMR terminals (white arrowheads). Piezo2-FLAG is not present within the cell bodies of TSC or lamellar cells (located at the base of the hair follicle and Meissner corpuscle, respectively) and is not observed above background tissue levels in the spherical cloud of lamellar cell processes within the Meissner corpuscle (S100B⁺) and Pacinian corpuscle (PLP^{EGFP}). Scalebar, 10 μ m.

(G) FLAG and NFH co-staining in wild-type littermates of *Piezo2^{smFP-FLAG}* animals performed side-by-side and processed with same confocal settings as Figure 1B. White arrowheads show location of NFH⁺ A β RA-LTMRs forming lanceolate endings and innervating the Meissner corpuscle and Pacinian corpuscle. Scalebar, 25 μ m.

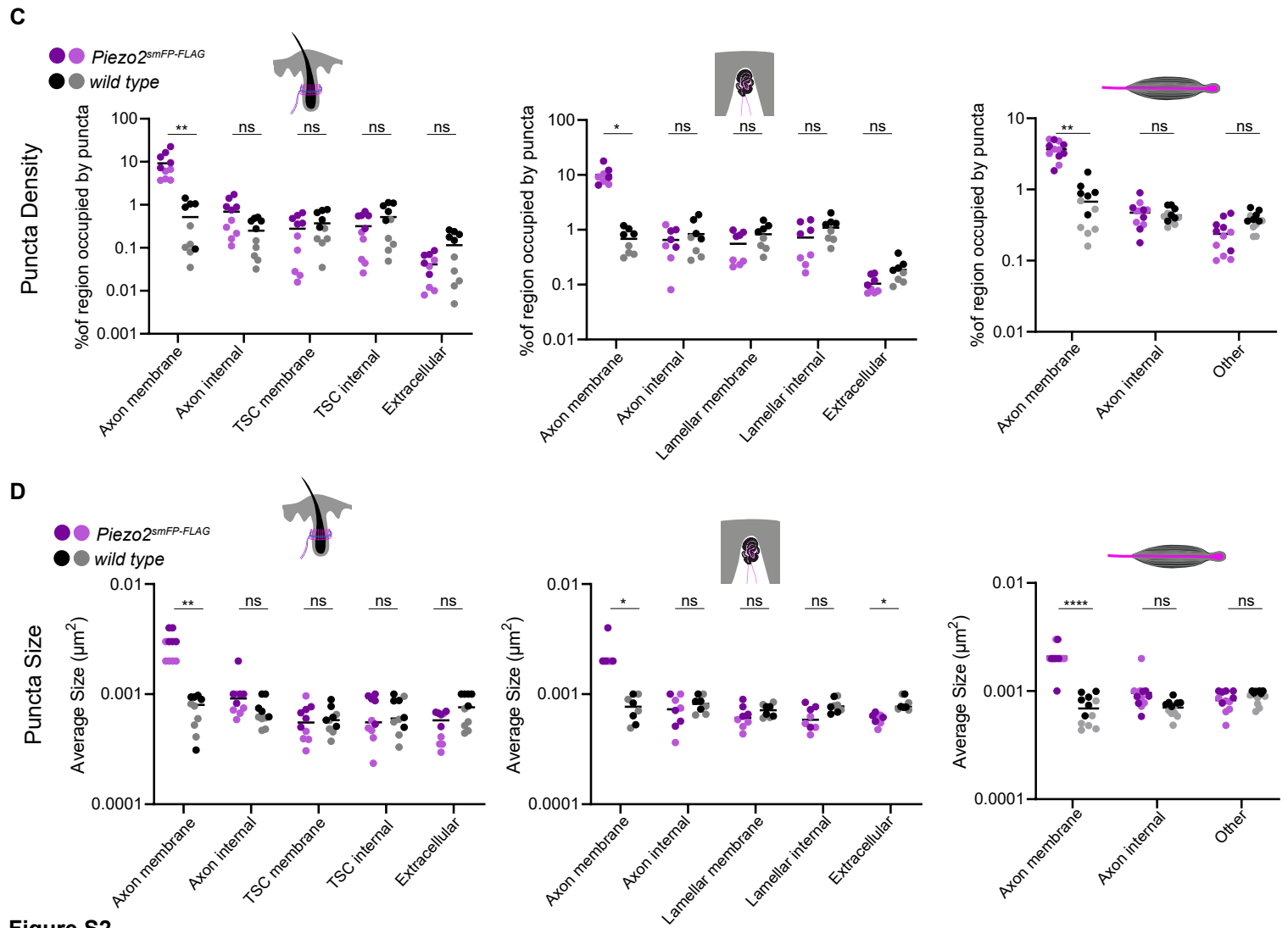
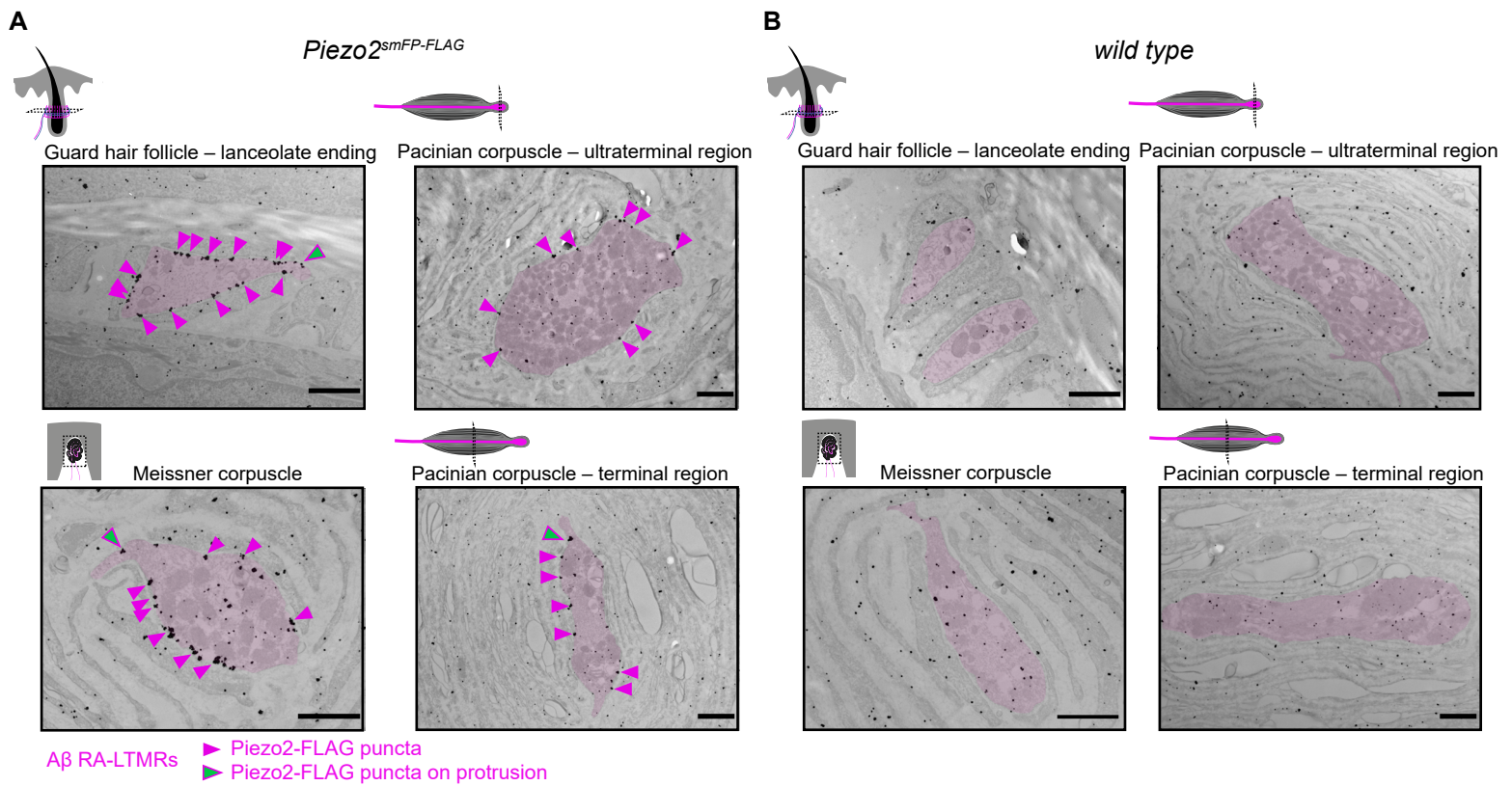


Figure S2

Figure S2. Additional examples of Piezo2 enrichment along the membrane of A β RA-LTMRs and quantification of Piezo2-FLAG puncta, related to Figure 1.

(A) Immuno-electron micrographs from a second *Piezo2*^{smFP-FLAG} animal stained for FLAG and processed with silver enhancement show enriched expression of the Piezo2-FLAG fusion protein along the axon membranes of the A β RA-LTMRs that form lanceolate endings around the hair follicle and innervate the Meissner corpuscle and Pacinian corpuscle within both the terminal and ultraterminal region (A β RA-LTMRs pseudo-colored pink). Piezo2-FLAG puncta can be seen along the sensory axon membranes (pink arrowheads) and along small cytoplasmic axon protrusions (green arrowheads). Not all puncta are labeled by arrowheads. Scalebar, 1 μ m.

(B) Immuno-electron micrographs from a wild-type littermate of the *Piezo2*^{smFP-FLAG} animal shown in (A) stained for FLAG and processed with silver enhancement. The A β RA-LTMRs of each end organ are pseudo-colored pink. Scalebar, 1 μ m.

(C) Quantification of puncta density (percentage of region occupied by puncta) within the guard hair lanceolate endings (left) and Meissner corpuscle (middle) of *Piezo2*^{smFP-FLAG} animals (dark purple/light purple) and littermate controls (black/gray) localized to the A β sensory axon membrane, A β sensory axon intracellular space (internal), terminal Schwann cell (TSC) or lamellar cell membrane, TSC or lamellar cell intracellular space (internal), and the extracellular space. (Right) Same quantification performed for the Pacinian corpuscle except due to the complexity, density and poor ultrastructural resolution of the lamellar cells within the terminal and ultraterminal region of the Pacinian corpuscle, the extracellular space and lamellar cell processes were grouped as “other”. Each dot represents the analysis of a single image and the different color shades represent images from each of the two separate experiments. The mean of each group is plotted. Statistical significance determined using the Kruskal-Wallis test with Dunn’s multiple comparisons test. *** $p \leq 0.001$, ** $p \leq 0.01$, * $p < 0.05$, ns ≥ 0.05 . N = 10, 8, 12 images for the hair follicle, Meissner corpuscle, and Pacinian corpuscle analysis, respectively. Data plotted on log scale.

(D) Same as in (C) except quantifying puncta size across the different subcellular locations of the guard hair lanceolate endings (left), Meissner corpuscle (middle), and Pacinian corpuscle (right).

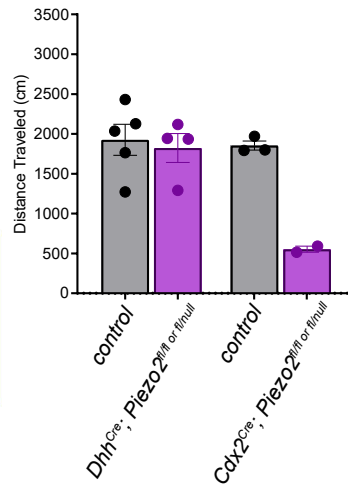
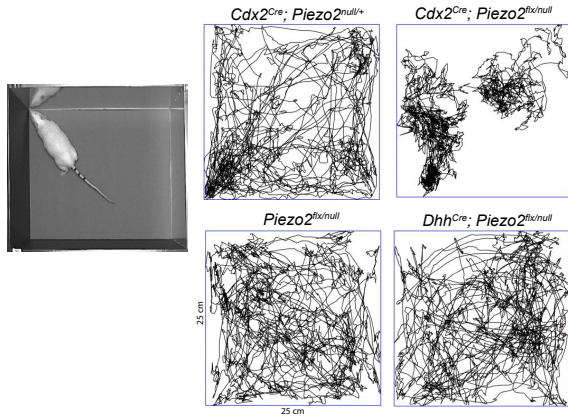
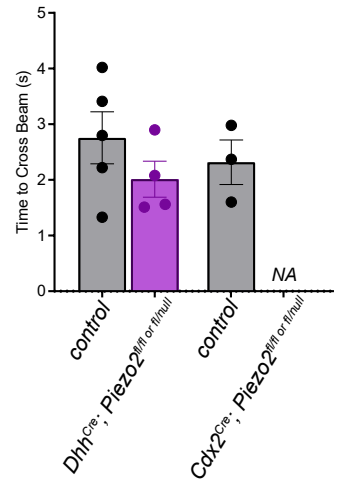
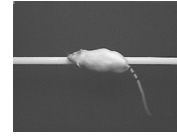
A**B****Figure S3**

Figure S3. Piezo2 is essential in sensory axons but dispensable in lamellar and terminal Schwann cells for coordinated ambulatory behaviors, related to Figure 2.

(A) Distance traveled in open field test for *Dhh^{Cre};Piezo2^{fl/fl or fl/-}* mice (selective deletion of Piezo2 in peripheral Schwann cells, n = 4) and littermate controls (n = 5), and for *Cdx2^{Cre};Piezo2^{fl/fl or fl/-}* mice (deletion of Piezo2 in peripheral Schwann cells and sensory neurons, n = 2) and littermate controls (n = 3). Representative movement traces for each genotype (control shown on left and mutant on right) is shown to the left of bar graph.

(B) Total time to cross balance beam for *Dhh^{Cre};Piezo2^{fl/fl or fl/-}* mice (n = 4) and littermate controls (n = 5), and littermate controls (n = 3) for the *Cdx2^{Cre};Piezo2^{fl/fl or fl/-}* mice.

Cdx2^{Cre};Piezo2^{fl/fl or fl/-} mice could not be tested on the balance beam assay due to their severe motor deficit.

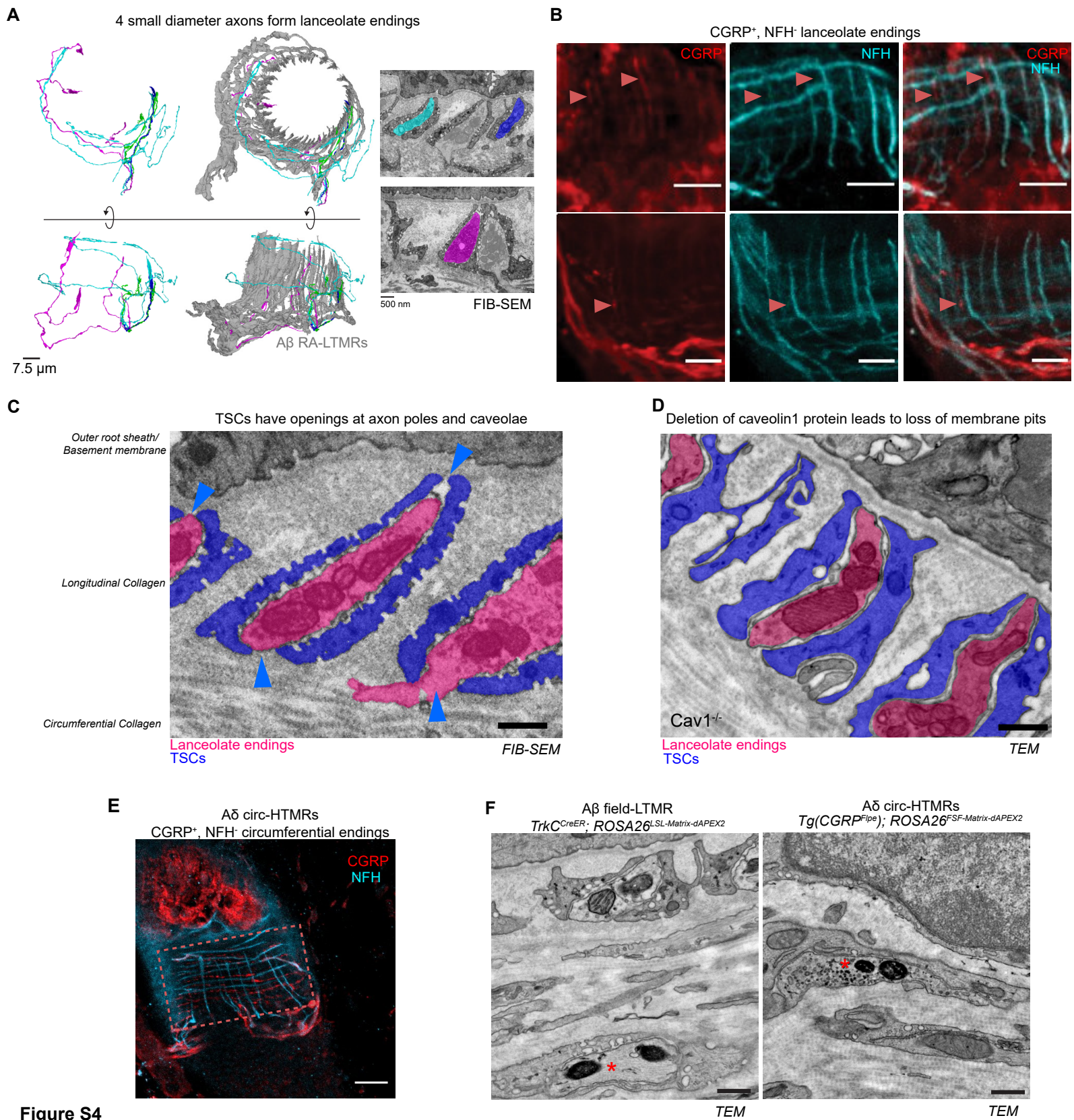


Figure S4

Figure S4. Further characterization of cellular and structural features of the guard hair follicle, related to Figure 4.

(A) 3D renderings of the six A β RA-LTMRs (gray) that form 47 lanceolate endings and four small caliber axons (magenta, green, cyan, and blue) that form six lanceolate endings around the guard hair. On right, single sections from the FIB-SEM volume with pseudo-colored lanceolate endings formed by A β RA-LTMRs and the small caliber neurons.

(B) CGRP and NFH staining of hairy skin reveals CGRP⁺, NFH⁻ lanceolate endings, marked by red arrowheads. Examples from two animals are shown. Scalebar, 10 μ m.

(C) Single section from FIB-SEM volume with pseudo-colored A β RA-LTMR lanceolate ending (magenta) and TSCs (blue). The membrane of TSCs contains cup-shaped caveolae. Blue arrowheads indicate the gaps in TSC coverage that form closest to the outer root sheath and at the boundary of the longitudinal and circumferential collagen matrix. Scalebar, 500 nm.

(D) Single section TEM of a hair follicle from a *Caveolin-1* knock-out animal with lanceolate endings pseudo-colored in magenta and TSCs pseudo colored in blue. This experiment was repeated in three animals. Scalebar, 500 nm.

(E) CGRP and NFH staining of hairy skin showing CGRP⁺, NFH⁻ circumferential endings of A δ circ-HTMRs. Scalebar, 20 μ m.

(F) Left, single section TEM showing mitochondrial dAPEX2 labeled A β field-LTMR (asterisk) from a *TrkC^{CreER}; ROSA26^{LSL-Matrix-dAPEX2}* animal treated with 0.5 mg of TAM at P5. Abundant neurofilaments were observed in these profiles. Right, single section TEM showing mitochondrial dAPEX2 labeled A δ circ-HTMR (asterisk) from a *Tg(CGRP-Flpe); ROSA26^{FSF-Matrix-dAPEX2}* animal. Neurofilaments were never found in these profiles, and these profiles tend to be smaller in diameter than A β field-LTMRs. Labeling was performed in one animal for each genotype. Scalebar, 500 nm.

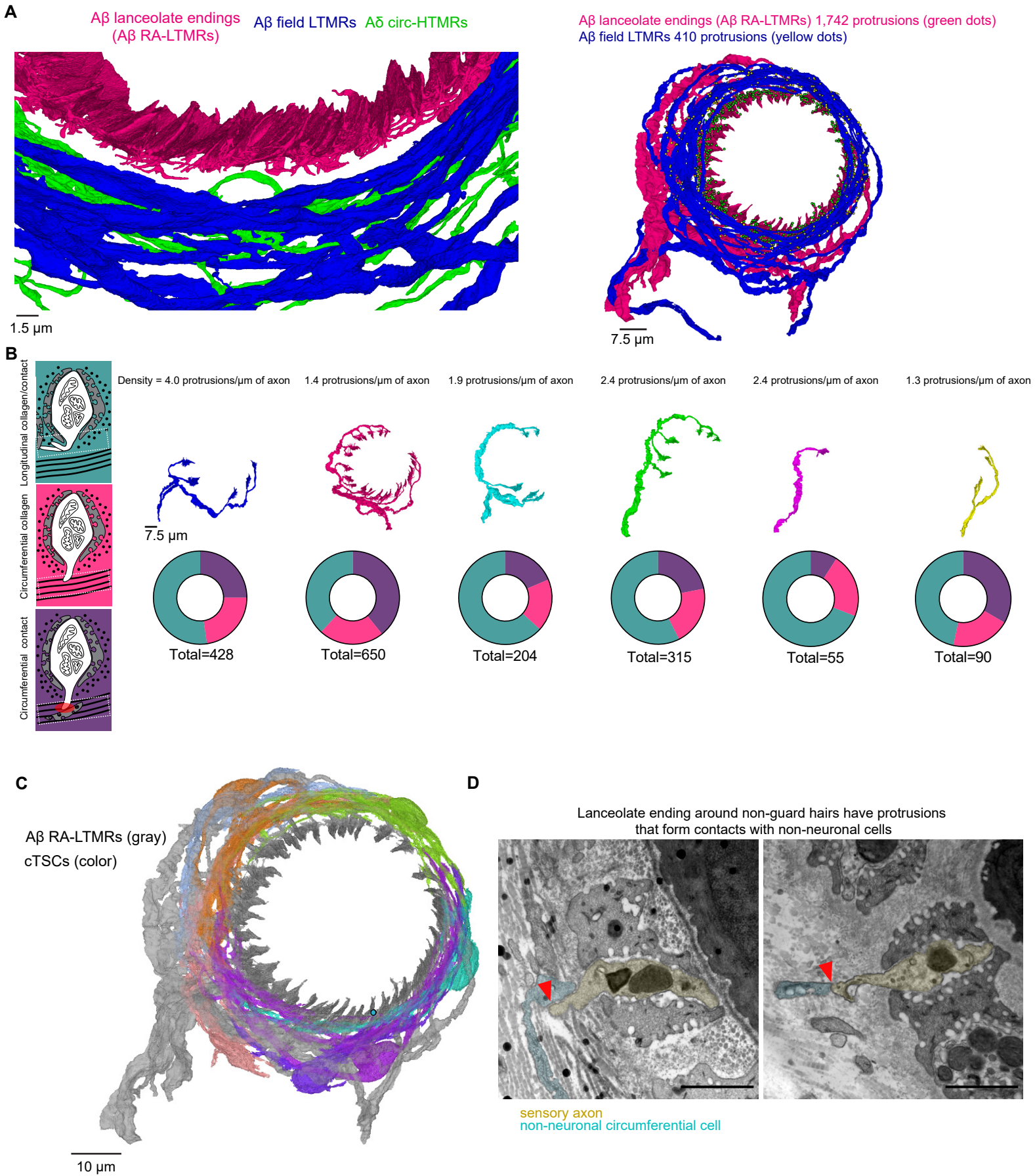


Figure S5

Figure S5. Axon protrusions are present along all A β RA-LTMR lanceolate endings and are minimally present along the less sensitive A β field LTMRs and A δ circ-HTMRs, related to Figure 5.

(A) Left, high magnification, 3D renderings from the guard hair FIB-SEM volume showing numerous axon protrusions along the A β RA-LTMR lanceolate endings (magenta) and the paucity of protrusions along the A β field-LTMRs (blue) and A δ circ-HTMRs (green). Right, 3D renderings showing all the protrusions along the A β RA-LTMR lanceolate endings (protrusions marked by green dots, A β RA-LTMRs rendered in magenta) and all the protrusions along the A β field-LTMRs (protrusions marked by yellow dots, A β field-LTMRs rendered in blue).

(B) Quantification of axon protrusions for each of the six A β RA-LTMR axon segments. The density of protrusions for each axon segment is noted. Left schematic shows the three different termination patterns quantified. Teal: protrusions that stay within the local longitudinal collagen matrix and either contact local TSCs or terminate within the longitudinal collagen without making contact. Magenta: protrusions that extend into the circumferential collagen matrix but do not contact cells in the circumferential collagen matrix. Purple: protrusions that extend into the circumferential collagen matrix and contact cells in the circumferential collagen matrix. A 3D rendering for each A β RA-LTMR is shown and the breakdown of protrusion terminal types is shown below.

(C) 3D rendering of A β RA-LTMRs in gray and circumferential TSCs (cTSCs) shown in color. A single teal dot marks the point of contact between an axon protrusion and a circumferential TSC.

(D) Two single section TEM images (processed with tannic acid and post-stained) from non-guard hairs showing axon protrusions of lanceolate-forming sensory axons (yellow) extending into the circumferential collagen network and contacting non-neuronal cells (blue). Scale bar, 1 μ m. Images were collected from one animal.

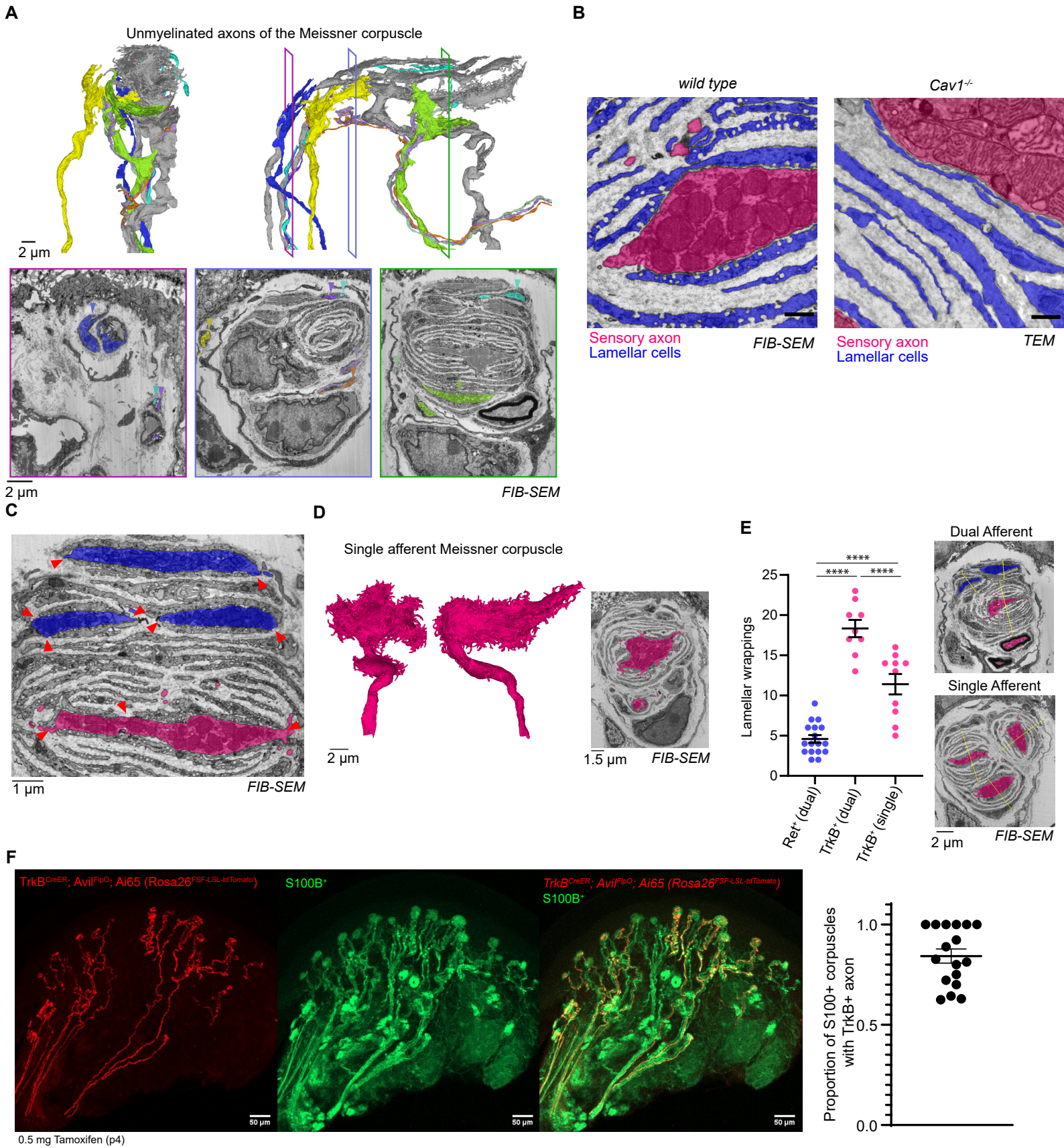


Figure S6

Figure S6. Further characterization of cellular and structural features of the Meissner corpuscle, related to Figure 6.

(A) 3D renderings of the two A β RA-LTMRs (shown in gray) and the seven (shown in color) small caliber/unmyelinated axons of the Meissner corpuscle. Three images taken from different depths of the Meissner corpuscle FIB-SEM volume show the pseudo-colored axon profiles of all seven small caliber/unmyelinated axons with arrowheads indicating their location.

(B) Left, single section from FIB-SEM volume with A β RA-LTMR pseudo-colored magenta and lamellar cell processes pseudo-colored blue. The membranes of lamellar cells contain cup-shaped caveolae. Right, single section TEM image of a Meissner corpuscle in a *Caveolin-1* knock-out animal shows the loss of caveolae in the lamellar cell processes. This loss of caveolae was observed in the Meissner corpuscles of two *Caveolin-1* knock-out animals. Scalebar, 500 nm.

(C) Single section from the FIB-SEM volume with the two A β RA-LTMRs shown in blue and magenta. Arrowheads indicate gaps in lamellar cell coverage of the sensory axons where axon protrusions often emerge.

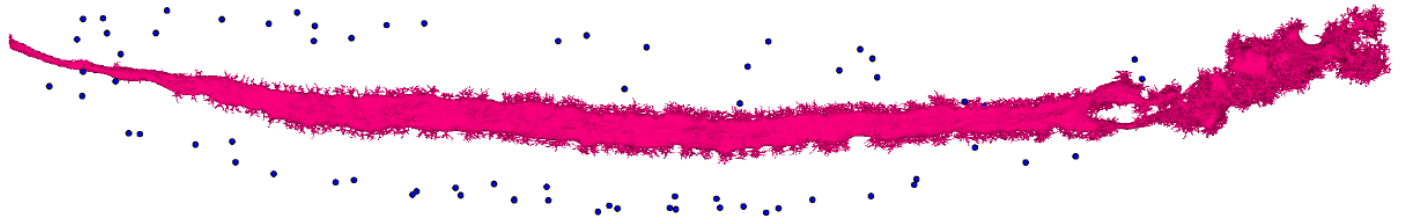
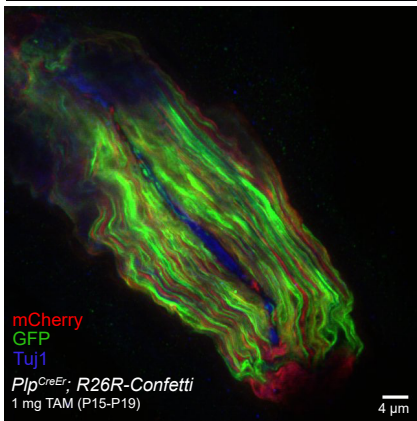
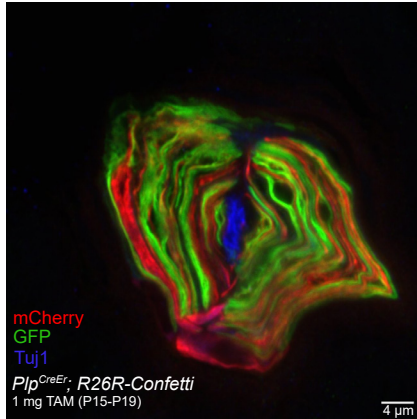
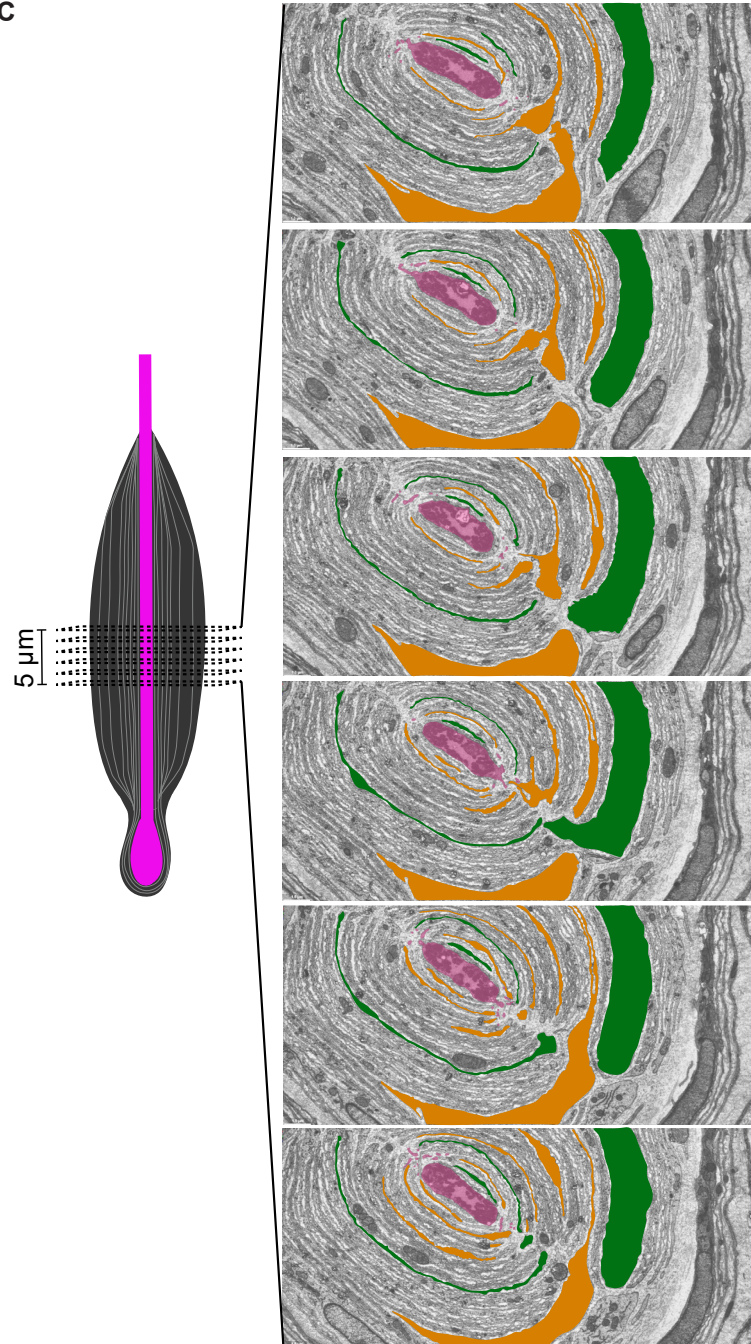
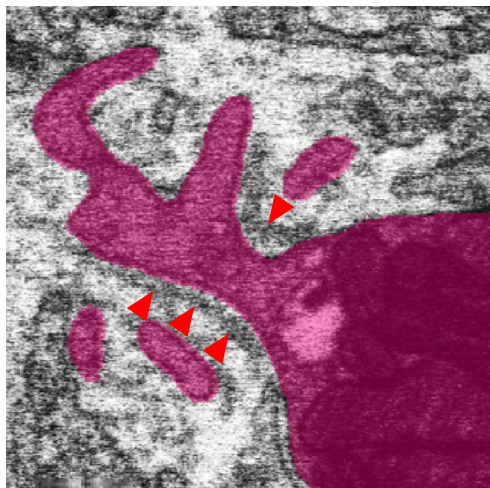
(D) Left, 3D rendering of the A β RA-LTMR reconstructed from the Meissner corpuscle with a single myelinated afferent. Right, a single section from the FIB-SEM volume with the A β RA-LTMR pseudo-colored in magenta.

(E) Quantification of the number of lamellar cell wrappings around the Ret⁺ and TrkB⁺ axon from the dual-innervated Meissner corpuscle volume and the TrkB⁺ axon from the single-innervated Meissner corpuscle volume. Each data point represents the number of lamellar cell wrappings associated with each sensory axon profile visualized in imaging planes distributed across both corpuscle volumes (9 planes were selected for the dual-innervated corpuscle, containing a total of 17 Ret⁺ axon profiles and 9 TrkB⁺ axon profiles, and 6 planes were selected for the single-innervated corpuscle, containing a total of 10 TrkB⁺ axon profiles). Example imaging planes for both volumes are shown on the right with the Ret⁺ axon pseudo-colored blue and the TrkB⁺ axons colored magenta. The yellow lines indicate the expanse of lamellar cell wrappings for each individual sensory axon profile. A one-way ANOVA revealed a statistically significant difference in lamellar wrappings between at least two groups ($F(2,33) = 64.87$, $p < 0.0001$. Tukey's test for multiple comparisons: **** $p \leq 0.0001$). Mean \pm SEM is plotted.

(F) Co-staining thick (200 μm) sections from *TrkB^{CreER}; Avil^{FlpO}; Ai65 (Rosa26^{FSF-LSL-tdTomato})* animals with mCherry and S100B was used to quantify the proportion of S100B⁺ Meissner corpuscles innervated by a TrkB⁺ axon. Each data point (n = 17) represents the proportion of corpuscles with a TrkB⁺ axon in a single 200 μm thick section. Mean \pm SEM is plotted. Sections were collected from two animals.

A

Position of lamellar cell bodies within the inner core

15 μm **B****C****D**

300 nm

Figure S7

Figure S7. Further characterization of cellular and structural features of the Pacinian corpuscle, related to Figure 7.

(A) 3D rendering of the A β RA-LTMR innervating the Pacinian corpuscle. The blue dots mark the position of the soma of the lamellar cells that make up the inner core.

(B) Cross section through the short (top) and long (bottom) axis of Pacinian corpuscles isolated from a *Plp^{CreER}; R26R^{Confetti}* mouse showing intermingled red and green processes from numerous lamellar cells. This experiment was performed in one animal.

(C) Six image planes distributed across 5 μ m of the Pacinian corpuscle FIB-SEM volume. A subset of lamellar cell processes originating from two distinct lamellar cells (orange and green) are traced across the six images to reveal the intermingled nature of lamellar cell processes within the Pacinian corpuscle volume.

(D) Single section from the FIB-SEM volume of the Pacinian corpuscle with the A β RA-LTMR pseudo-colored magenta. Red arrowheads mark collagen fibers that surround the base of protrusions.

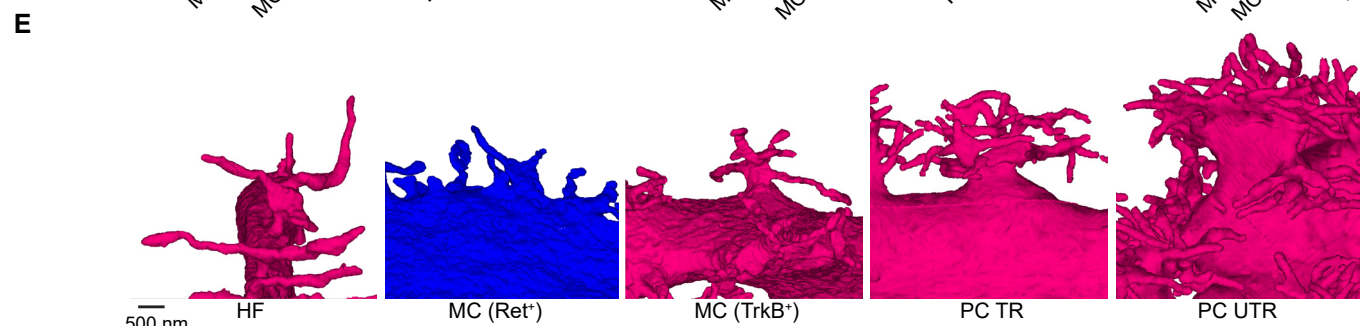
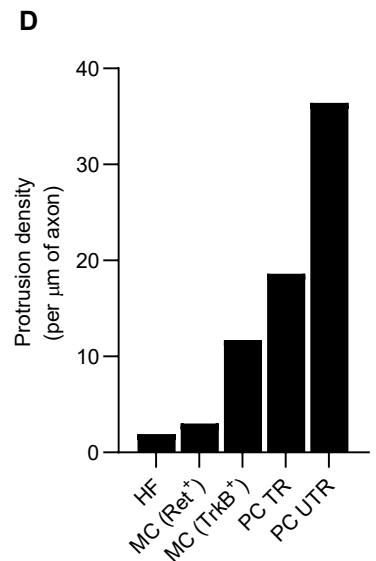
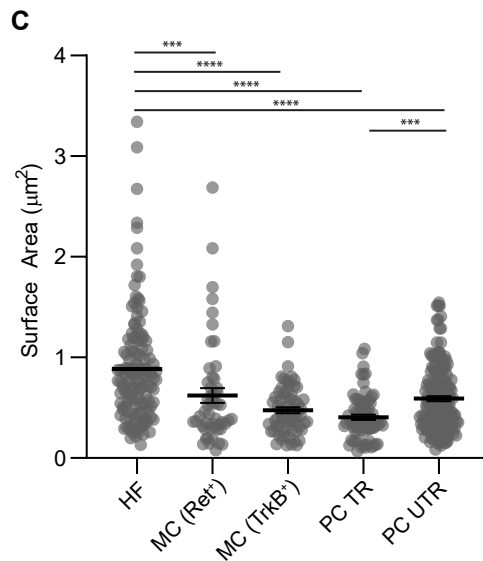
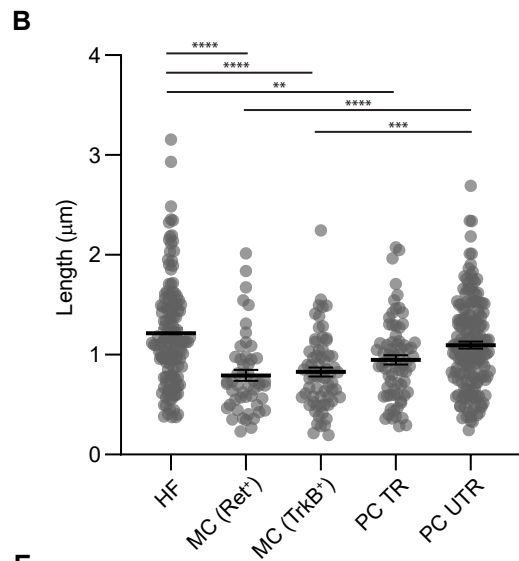
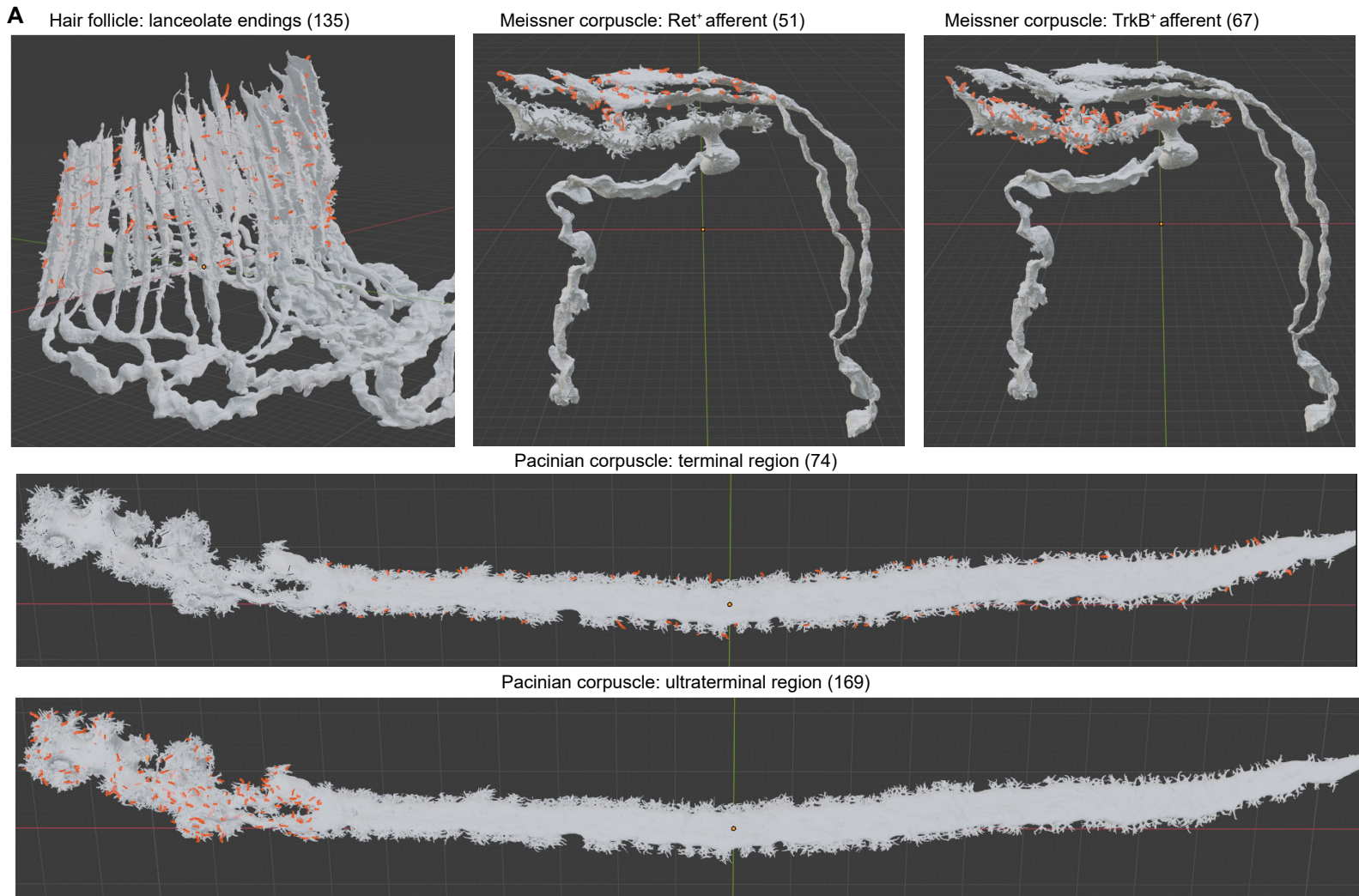


Figure S8

Figure S8. Morphometric analysis of A β LTMR axon protrusions across end organ structures, related to Figure 8.

(A) 3D renderings showing the subset of axon protrusions (highlighted in orange) analyzed along the A β LTMR sensory axons (white) of the guard hair follicle, Meissner corpuscle (dual-innervated) and the Pacinian corpuscle FIB-SEM volumes (within both the terminal and ultraterminal region).

(B) Quantification of the length of analyzed axon protrusions selected from the A β RA-LTMR lanceolate endings around the guard hair follicle (HF), the A β LTMR Ret⁺ axon (MC Ret⁺) and the A β RA-LTMR TrkB⁺ axon (MC TrkB⁺) of the dual-innervated Meissner corpuscle, and the terminal region (PC TR) and ultraterminal region (PC UTR) of the A β RA-LTMR axon innervating the Pacinian corpuscle. Each dot represents an individual axon protrusion. Statistical significance determined using the Kruskal-Wallis test with Dunn's multiple comparisons test. **** $p \leq 0.0001$, *** $p \leq 0.001$, ** $p \leq 0.01$. Mean \pm SEM is plotted, $n = 135$ (HF), 51 (MC Ret⁺), 67 (MC TrkB⁺), 74 (PC TR), 169 (PC UTR).

(C) Same as in (B) except for quantification of axon protrusion surface area.

(D) Protrusion density for the A β LTMR sensory axons forming the lanceolate endings around the guard hair follicle (HF), the Ret⁺ (MC Ret⁺) and TrkB⁺ (MC TrkB⁺) axons of the dual-innervated Meissner corpuscle and the terminal (PC TR) and ultraterminal (PC UTR) region of the Pacinian corpuscle (estimated).

(F) 3D renderings of the A β LTMR sensory axons forming the lanceolate endings around the guard hair follicle (HF), the Ret⁺ (MC Ret⁺) and TrkB⁺ (MC TrkB⁺) axons of the dual-innervated Meissner corpuscle and the terminal (PC TR) and ultraterminal (PC UTR) region of the Pacinian corpuscle showing the varied branching pattern across A β LTMR sensory axon types and end organ structures.